Article

Not peer-reviewed version

# Mathematical Modeling, Control, and Simulation of Active Suspension System for a Quarter Car Model

Sultan Mahamdnur Ibrahim * and Yohanis Dabesa Jelila

Posted Date: 5 March 2026

doi: 10.20944/preprints202603.0358.v1

Keywords: active suspension system; mathematical modeling; state-space form; PID controller

Preprints.org (www.preprints.org) | NOT PEER-REVIEWED | Posted: 5 March 2026 doi:10.20944/preprints202603.0358.v1



*Article*

# Mathematical Modeling, Control, and Simulation of Active Suspension System for a Quarter Car Model

**Sultan Mahamdnur Ibrahim [1,*] and Yohanis Dabesa Jelila [2]**

[1] Faculty of Mechanical and Industrial Engineering, Aksum Institute of Technology, Aksum University, Ethiopia

[2] Faculty of Mechanical Engineering, Jimma Institute of Technology, Jimma University, P.O. Box 378, Ethiopia

* Correspondence: sultanmhmdnr@gmail.com

**Abstract**

The suspension system plays a significant role in ride comfort, car weight support, and road handling, which is crucial for the safety of the ride. This paper illustrates a derivation of a mathematical model and proportional-integral-derivative (PID) controller design for an active suspension system for a quarter car model of a passenger car. The performance of an active suspension system in terms of the vertical acceleration of the car body, suspension deflection, and tyre deflection is compared with that of a passive suspension system when subjected to road disturbance. The results show that the active suspension system with PID controller provides better performance compared to that of the passive suspension system.

**Keywords:** active suspension system; mathematical modeling; state-space form; PID controller

---

## 1. Introduction

Nowadays, the crucial problem facing the world's society is road traffic accidents. The number of people killed in road traffic crashes each year is estimated to be 1.2 million, while the number injured could be more than 50 million [1]. There are multiple factors contributing to the incidence of road traffic accidents, including human factors (road users and drivers' errors), environmental factors, and vehicle defect factors. Vehicle defect factors include suspension and steering systems, brakes, tyres/wheels, engine, transmission, windows or vision, and lights [2–6].

The suspension system, which connects the vehicle chassis to axle-wheel-tyre assemblies, plays a key role in ride comfort, vehicle weight support, and road handling which is crucial for the safety of the ride. Ride comfort can be defined as the ability of the vehicle suspension system to insulate passengers (and loads) from vibrations caused by road surface irregularities. The physical quantity that relates ride comfort to the suspension system is the vertical acceleration of the vehicle body [7]. The weight support ability of the vehicle depends on the suspension travel (suspension deflection), which represents the relative displacement between the vehicle body and the axle-wheel-tyre assemblies. Vehicle weight can be supported by maintaining minimum suspension deflection because the suspension deflection is limited by the mechanical structure [8]. Road handling refers to the road holding ability in different types of vehicle maneuvering conditions, such as cornering, accelerating, or braking. The physical quantity that relates road handling ability to the suspension system is the tyre deflection [9]. Road handling is achieved if tyres are kept in contact with the road with minimal tyre deflection.

Suspension systems can be classified into three categories: passive, semi-active, and active suspension systems. The passive suspension system consists mainly of a spring and a viscous damper. The spring is used to store energy, while the viscous damper is used to dissipate energy. The parameters of the passive suspension system elements are fixed. This has affected vehicle ride comfort and road handling performances. The semi-active suspension system is similar to the passive suspension system, but the viscous damper is controlled to dissipate energy [10–12]. In an active suspension system, with additional components such as sensors and controllers, an actuator (pneumatic, hydraulic, or electromagnetic) is placed in parallel with passive elements: a spring and viscous damper. The actuator is capable of adding energy to the suspension system [13–16]. The energy added by the actuator is controlled based on the states of the vehicle, which are acquired from various sensors located at different points of the vehicle.

A passive suspension system is designed to preserve two desired performances, which are passenger ride comfort and road handling ability. A design problem is to provide a tradeoff between both performances that are opposite to one another. In active suspension system design, the primary goal is to resolve the inherent tradeoffs among passenger ride comfort and road handling ability by using an actuator that is controlled. Hence, an active suspension system can provide a high level of ride comfort by isolating the vehicle chassis from road disturbances and improving road handling by preventing the tyre from losing road contact.

Various control strategies have been proposed to control the actuator of the active suspension system, such as linear optimal control [17], adaptive control [18], $H_\infty$ control [19], fuzzy logic control [20], and neural network control [21]. In this paper, PID control is used due to its simplicity, robustness, and effectiveness in a wide range of practical applications.

This paper focuses on deriving a mathematical model and designing a PID controller for an active suspension system for a passenger car to illustrate its potential for improving ride comfort and road handling ability. A quarter car model is used to observe the performance of a car suspension system in terms of the vertical acceleration of the car body, suspension deflection, and tyre deflection when subjected to road disturbances.

The remaining parts of the paper are organized as follows: in Section 2, an active suspension system for a quarter car model is described, and its mathematical model is derived. Also, the mathematical model of the road profile is presented in Section 3. The PID control strategy for an active suspension system is presented in Section 4. In Section 5, the simulation results of active and passive suspension systems are given and discussed. Finally, conclusions are given in Section 6.

## 2. Mathematical Modeling

A quarter car model with 2 degree-of-freedom (DOF) shown in Figure 1 is used for mathematical model and simulation purposes of the suspension system. The mass of one-fourth of the car body represented by sprung mass $m_s$, and the mass of the axle-wheel-tyre assemblies is represented by unsprung mass $m_u$. The car body such that sprung mass $m_s$ is supported by a suspension system consisting of a linear spring, a viscous damper, and actuator force. The spring and viscous damper are characterized by stiffness coefficient $k_s$ and damping coefficient $c_s$. An actuator force $f(t)$ is represented by a linear hydraulic actuator that is modeled as an ideal force generator in the active suspension system and controlled by a controller using data of a road profile from a sensor attached to the car. The elastic and damping properties of the tyre are represented by the spring with stiffness coefficient $k_t$ and the damper with damping coefficient $c_t$. In this study, there is only vertical displacement input due to the road disturbance denoted by $z_r(t)$. It is assumed that the tyre is always in contact with the road.

doi:10.20944/preprints202603.0358.v1



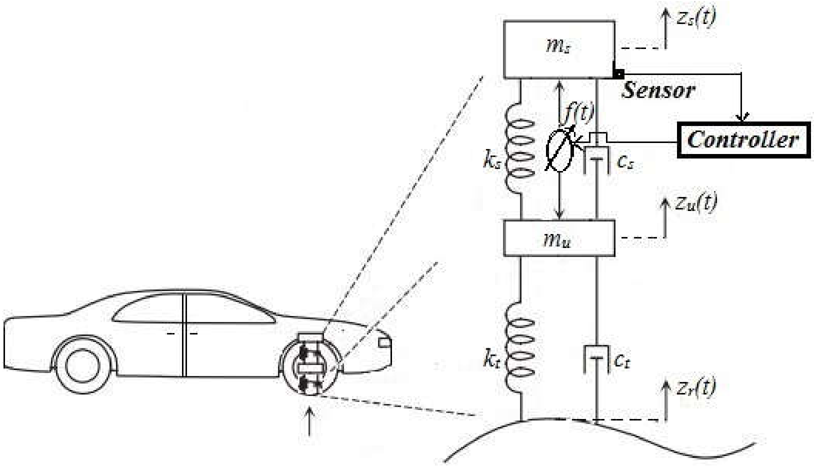


**Figure 1.** Physical system of a quarter car model for an active suspension system with sensor and controller.

The vertical displacements of the two masses $z_s(t)$ and $z_u(t)$ are chosen to be the generalized coordinates. Therefore, the static equilibrium positions of the two masses $m_s$ and $m_u$ are set as the coordinate origins. Now, assume that the vertical displacements are

$$z_s(t) > z_u(t) > z_r(t) > 0 \quad (1)$$

which implies that the springs are in tension and the elongation of the spring of the suspension system $k_s$ is $z_s(t) - z_u(t)$. Therefore, the force exerted by the spring of the suspension system $k_s$ on the sprung mass $m_s$ is downward as it tries to restore to the undeformed position. Because of Newton's third law, the force exerted by the spring of suspension system $k_s$ on the unsprung mass $m_u$ has the same magnitude, but opposite in direction. If the vertical displacements derivatives with respect to time, Eq. (1) becomes.

$$\dot{z}_s(t) > \dot{z}_u(t) > \dot{z}_r(t) > 0 \quad (2)$$

which implies the sprung mass $m_s$ moves faster than the unsprung mass $m_u$ and the motion of the damper of the suspension system $c_s$ is $\dot{z}_s(t) - \dot{z}_u(t)$. Therefore, the force exerted by the damping of the suspension system $c_s$ on the sprung mass $m_s$ is downward as it tries to oppose the motion of the sprung mass $m_s$. Again, because of Newton's third law the force exerted by the damping of suspension system $c_s$ on the unsprung mass $m_u$ has the same magnitude, but opposite in direction. The forces of the spring of the tyre $k_t$ and damping of the tyre $c_t$ can be obtained using the same concept. So, the Free-Body-Diagram (FBD) of sprung mass $m_s$ and unsprung mass $m_u$ is shown in Figure 2.

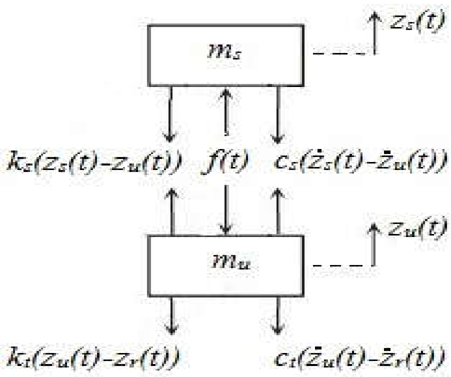


**Figure 2.** FBD of quarter car model active suspension system.

 doi:10.20944/preprints202603.0358.v1



It is important to note that the gravitational forces $m_s g$ and $m_u g$ (where $g$ is gravitational acceleration) are not included in the FBD because the static equilibrium positions of masses $m_s$ and $m_u$ are chosen as the coordinate origins.

Applying Newton's second law to the masses $m_s$ and $m_u$ using Eq. (3) to obtain the differential equations of motion Eq. (4) and (5) as following,

$$ma_z(t) = {}^{+}\!\uparrow z \sum F_z(t) \tag{3}$$

For sprung mass $m_s$:

$$m_s \ddot{z}_s(t) = -k_s\left(z_s(t) - z_u(t)\right) + f(t) - c_s\left(\dot{z}_s(t) - \dot{z}_u(t)\right) \tag{4}$$

For unsprung mass $m_u$:

$$m_u \ddot{z}_u(t) = k_s\left(z_s(t) - z_u(t)\right) - f(t) + c_s\left(\dot{z}_s(t) - \dot{z}_u(t)\right) - k_t\left(z_u(t) - z_r(t)\right) - c_t\left(\dot{z}_u(t) - \dot{z}_r(t)\right) \tag{5}$$

Rearranging these differential equations (Eq. (4) and (5)) into input-output form as

$$m_s \ddot{z}_s(t) + c_s \dot{z}_s(t) - c_s \dot{z}_u(t) + k_s z_s(t) - k_s z_u(t) = f(t) \tag{6}$$

$$m_u \ddot{z}_u(t) - c_s \dot{z}_s(t) + (c_s + c_t)\dot{z}_u(t) - k_s z_s(t) + (k_s + k_t) z_u(t) = -f(t) + k_t z_r(t) + c_t \dot{z}_r(t) \tag{7}$$

Now, representing these differential equations (Eq. (6) and (7)) of suspension system in state-space form. State-space form is an alternative mathematical representation of a system as a set of input, output, and state variables related by first-order differential equations. Assume the state variables which define the values of the output variables are

$$\begin{aligned} x_1(t) &= z_s(t) \\ x_2(t) &= z_u(t) \\ x_3(t) &= \dot{z}_s(t) \\ x_4(t) &= \dot{z}_u(t) \end{aligned} \tag{8}$$

The derivative of these state variables (Eq. (8)) with respect to time are state-variable equations and obtained as

$$\begin{aligned} \dot{x}_1(t) &= \dot{z}_s(t) \\ \dot{x}_2(t) &= \dot{z}_u(t) \\ \dot{x}_3(t) &= \ddot{z}_s(t) \\ \dot{x}_4(t) &= \ddot{z}_u(t) \end{aligned} \tag{9}$$

where $\dot{z}_s(t)$ and $\dot{z}_u(t)$ of the state-variable equations (Eq. (9)) obtained from the state variables (Eq. (8)) as

$$\begin{aligned} \dot{z}_s(t) &= x_3(t) \\ \dot{z}_u(t) &= x_4(t) \end{aligned} \tag{10}$$

By using Eq. (8) and (10); $\ddot{z}_s(t)$ and $\ddot{z}_u(t)$ of the state-variable equations (Eq. (9)) obtained from the equation of motion Eq. (6) and (7), respectively, as

$$m_s \ddot{z}_s(t) + c_s x_3(t) - c_s x_4(t) + k_s x_1(t) - k_s x_2(t) = f(t) \tag{11}$$

$$m_u \ddot{z}_u(t) - c_s x_3(t) + (c_s + c_t) x_4(t) - k_s x_1(t) + (k_s + k_t) x_2(t) = -f(t) + k_t z_r(t) + c_t \dot{z}_r(t) \tag{12}$$

Rearranging Eq. (11) and (12) as

$$\ddot{z}_s(t) = -\frac{k_s}{m_s} x_1(t) + \frac{k_s}{m_s} x_2(t) - \frac{c_s}{m_s} x_3(t) + \frac{c_s}{m_s} x_4(t) + \frac{1}{m_s} f(t) \tag{13}$$

 doi:10.20944/preprints202603.0358.v1



$$\ddot{z}_u(t)=\frac{k_s}{m_u}x_1(t)-\frac{(k_s+k_t)}{m_u}x_2(t)+\frac{c_s}{m_u}x_3(t)-\frac{(c_s+c_t)}{m_u}x_4(t)-\frac{1}{m_u}f(t)+\frac{k_t}{m_u}z_r(t)+\frac{c_t}{m_u}\dot{z}_r(t) \quad (14)$$

Using Eq. (10), (13), and (14); the state-variable equations (Eq. (9)) become

$$\begin{aligned}
\dot{x}_1(t)&=x_3(t)\\
\dot{x}_2(t)&=x_4(t)\\
\dot{x}_3(t)&=-\frac{k_s}{m_s}x_1(t)+\frac{k_s}{m_s}x_2(t)-\frac{c_s}{m_s}x_3(t)+\frac{c_s}{m_s}x_4(t)+\frac{1}{m_s}f(t)\\
\dot{x}_4(t)&=\frac{k_s}{m_u}x_1(t)-\frac{(k_s+k_t)}{m_u}x_2(t)+\frac{c_s}{m_u}x_3(t)-\frac{(c_s+c_t)}{m_u}x_4(t)-\frac{1}{m_u}f(t)+\frac{k_t}{m_u}z_r(t)+\frac{c_t}{m_u}\dot{z}_r(t)
\end{aligned} \quad (15)$$

Rewriting this state-variable equation (Eq. (15)) into state-equation as

$$\dot{\mathbf{x}}(\mathbf{t})=A\mathbf{x}(\mathbf{t})+B\mathbf{u}(\mathbf{t})+G\mathbf{w}(\mathbf{t}) \quad (16)$$

Whereas,

$$\mathbf{x}(\mathbf{t})=\begin{Bmatrix}x_1(t)\\x_2(t)\\x_3(t)\\x_4(t)\end{Bmatrix}, \qquad A=\begin{pmatrix}0&0&1&0\\0&0&0&1\\-\frac{k_s}{m_s}&\frac{k_s}{m_s}&-\frac{c_s}{m_s}&\frac{c_s}{m_s}\\\frac{k_s}{m_u}&-\frac{(k_s+k_t)}{m_u}&\frac{c_s}{m_u}&-\frac{(c_s+c_t)}{m_u}\end{pmatrix}$$

$$\mathbf{u}(\mathbf{t})=\{f(t)\}, \qquad B=\begin{pmatrix}0\\0\\\frac{1}{m_s}\\-\frac{1}{m_u}\end{pmatrix}$$

**x(t)** is the state vector, **u(t)** is the input vector of controlled force (which represents only one actuator force, *f*(*t*)), and **w(t)** is the input vector of road disturbance. A is the state matrix, and B and G are the input matrices for input vectors **u(t)** and **w(t)**, respectively.

An active suspension system in this paper shows that passenger ride comfort can be improved by attaching only one sensor to the sprung mass $m_s$ of the quarter car model (Figure 1). So, it is assumed that only the sprung mass vertical displacement $z_s(t)$ could be measured (output) and used by the controller. The output $z_s(t)$ is $x_1(t)$ from the state variables (Eq. (8)). So, the output equation can be written in matrix from as:

$$\{y_1(t)\}=\begin{pmatrix}1&0&0&0\end{pmatrix}\begin{Bmatrix}x_1(t)\\x_2(t)\\x_3(t)\\x_4(t)\end{Bmatrix}+(0)\{f(t)\}+\begin{pmatrix}0&0\end{pmatrix}\begin{Bmatrix}z_r(t)\\\dot{z}_r(t)\end{Bmatrix} \quad (17)$$

As a result, the output equation can be conveniently expressed as

$$\mathbf{y}(\mathbf{t})=C\mathbf{x}(\mathbf{t})+D\mathbf{u}(\mathbf{t})+H\mathbf{w}(\mathbf{t}) \quad (18)$$

Where

$$C=\begin{pmatrix}1&0&0&0\end{pmatrix}$$

doi:10.20944/preprints202603.0358.v1



$$D = (0)$$

$$H = (0 \quad 0)$$

C is the output matrix, D and H are direct transmission matrices for input vectors **u(t)** and **w(t)**, respectively. It should be noted that the combination of the state equation (Eq. (16)) and output equation (Eq. (18)) is known as the state-space form [22].

$$\begin{aligned} \dot{\mathbf{x}}(\mathbf{t}) &= A\mathbf{x}(\mathbf{t}) + B\mathbf{u}(\mathbf{t}) + G\mathbf{w}(\mathbf{t}) \\ \mathbf{y}(\mathbf{t}) &= C\mathbf{x}(\mathbf{t}) + D\mathbf{u}(\mathbf{t}) + H\mathbf{w}(\mathbf{t}) \end{aligned} \tag{19}$$

A Simulink block diagram representation of state-space form (Eq. (19)) for a quarter car model active suspension system is shown below in Figure 3. In a passive suspension system, the actuator force or control input **u(t)** in Eq. (19) can be set to zero.

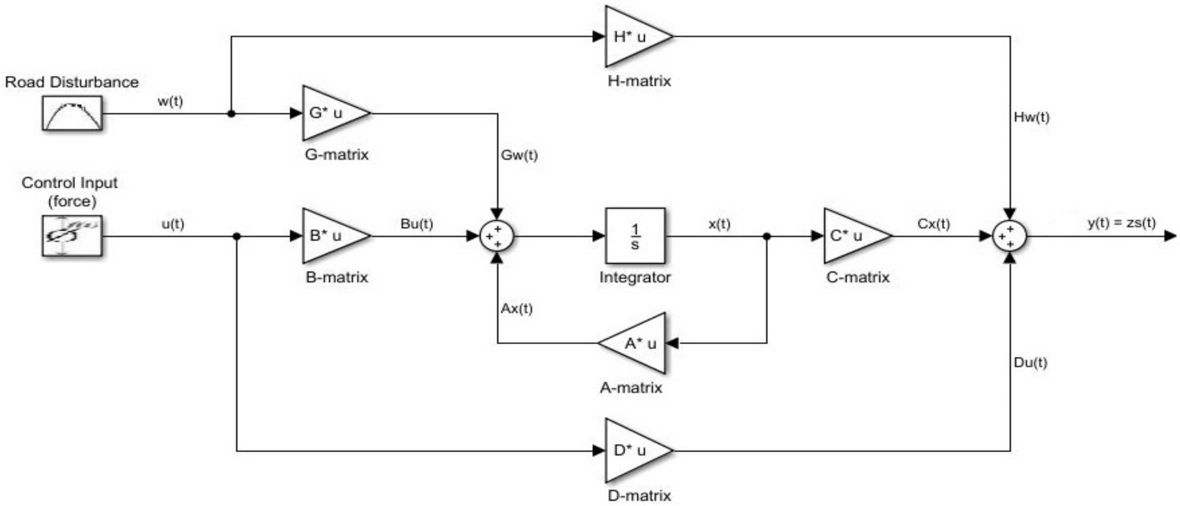


**Figure 3.** Simulink block diagram representation of state-space form.

The suspension system parameter values of the quarter car model used for simulation are given in Table 1.

**Table 1.** Quarter car model parameters [18].

| Parameter | Value | Units |
|---|---|---|
| $m_s$ | 290 | kg |
| $c_s$ | 1000 | N.s.m$^{-1}$ |
| $k_s$ | 16812 | N.m$^{-1}$ |
| $m_u$ | 59 | kg |
| $c_t$ | 0 | N.s.m$^{-1}$ |
| $k_t$ | 190000 | N.m$^{-1}$ |

The suspension deflection $z_s(t) - z_u(t)$ of the car is limited by the mechanical structure, and it is limited to $\pm 8cm$ [23].

## 3. Road Profile

A speed breaker road profile such as a single sinusoidal bump (Figure 5) was assumed as the road disturbance to the system. This road disturbance $z_r(t)$ is given by the expression [8,24],

$$z_r(t) = \frac{a}{2}\begin{cases}\left(1-\cos\left(\frac{2\pi v}{l}t\right)\right), & for\ \ t_1 \le t \le t_2 \\ 0, & else\end{cases} \tag{20}$$

Where $a$ is the height and $l$ is the width of bump of the road disturbance profile experienced by the wheel during a car travel with a constant forward speed $v$. $t$ represents the time and $t_1$ and $t_2$ are the time start and leave for the wheel contact with bump, and the time leave $t_2$ is given by,

$$t_2 = t_1 + \frac{l}{v} \tag{21}$$

The parameter values of the bump profile are $a = 0.05m$ and $l = 3.5m$, and the constant forward speed is $v = 25km.h^{-1}$. For a simulation time *6 seconds*, assuming the bump (speed breaker road profile) occur after $t_1 = 0.5$ *seconds*. A Simulink block diagram representation of road disturbance (Eq. (20)) is shown below in Figure 4.

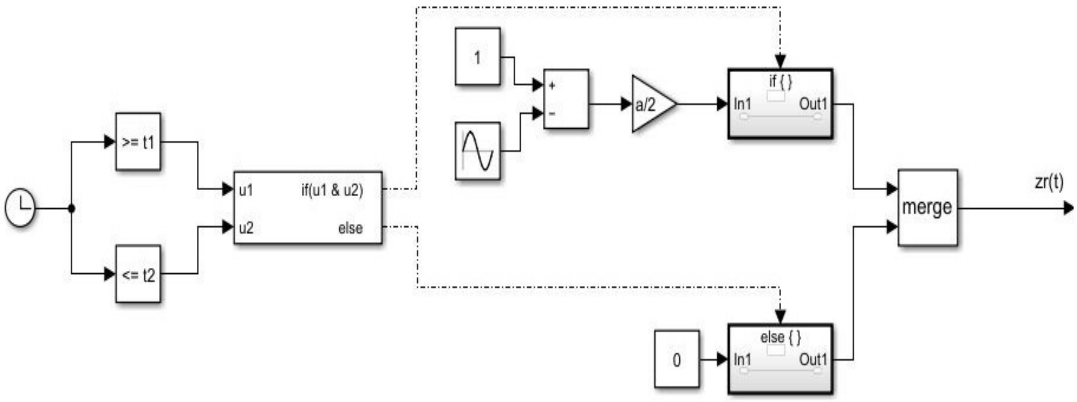


**Figure 4.** Simulink block diagram representation of road disturbance.

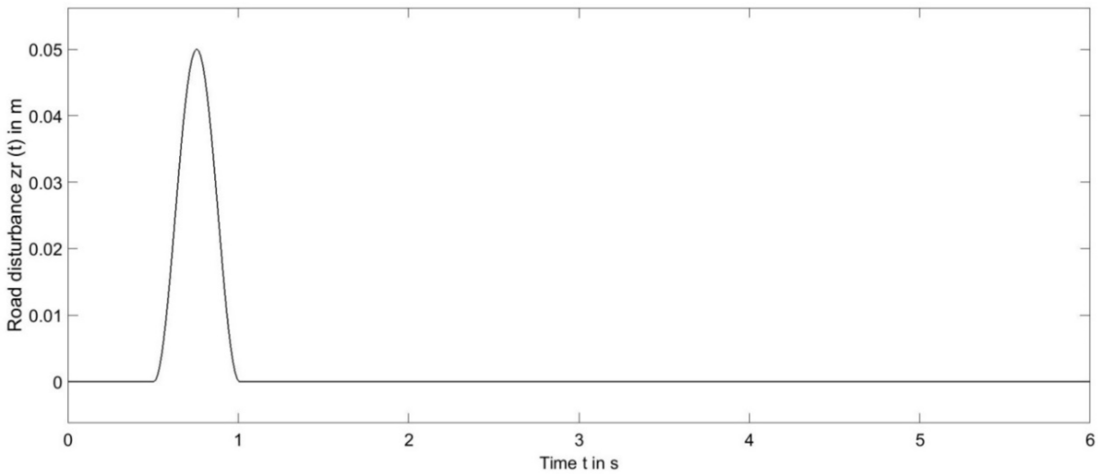


**Figure 5.** Road disturbance.

## 4. PID Controller Design

PID control is the most widely used control strategy in industrial control systems [25,26] because it is relatively simple to implement and tune, robust, and can provide stable control across a wide range of operating conditions. It consists of proportional *P(e(t))*, integral *I(e(t))*, and derivative *D(e(t))* parts. These parts can be interpreted in terms of time, as *P* depends on the present error, *I* on the accumulation of the past error, and *D* on the prediction of the future error. The weight sum of these

Preprints.org (www.preprints.org) | NOT PEER-REVIEWED | Posted: 5 March 2026 doi:10.20944/preprints202603.0358.v1



three parts is used to reduce the error to zero or a small value for the plant via a control element. The strength of the PID control strategy depends on the factors of the performance index, which can be weighted according to the designer's desires or other constraints using it.

Figure 6 shows a Simulink block diagram representation of an active suspension system for a quarter car model using a PID controller with feedback.

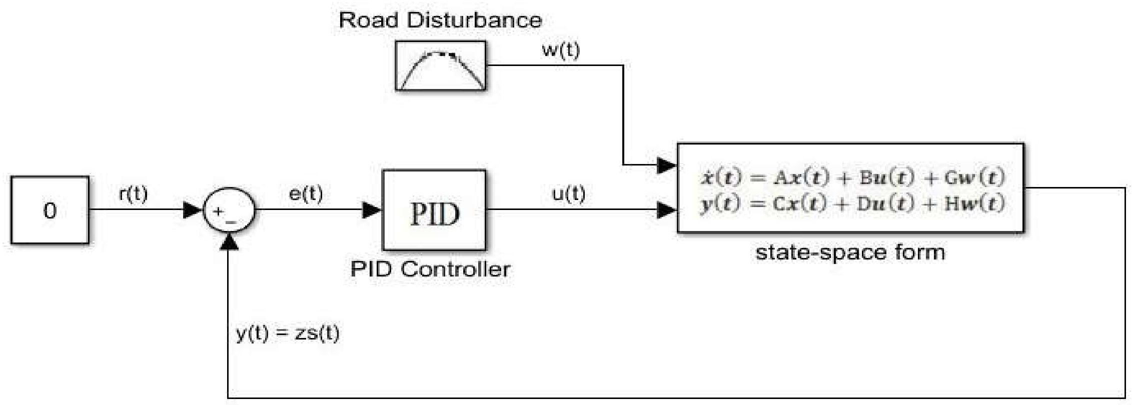


**Figure 6.** Simulink block diagram representation of active suspension system using PID controller with feedback.

In this paper, a sensor selected to measure the sprung mass vertical displacement $z_s(t)$, which is an output **y(t)** of the suspension system. This measurement from the sensor is sent without any time delay to compare it with the desired vertical displacement of the sprung mass *r(t)* in order to determine the error *e(t)*. The desired vertical displacement of the sprung mass *r(t)* is set to zero, and the error *e(t)* is represented as the input of the PID controller.

$$e(t) = r(t) - z_s(t) \tag{22}$$

With this error *e(t)*, the output of the PID controller can be given as [2,22],

$$\mathbf{u}(\mathbf{t}) = K_p e(t) + K_i \int_0^T e(t)dt + K_d \frac{de(t)}{dt} \tag{23}$$

Where, $K_p$ is proportional gain, $K_i$ is the integral gain, and $K_d$ is the derivatives gain and these gains known as controller parameters. Then, an input-controlled force **u(t)** is delivered to the quarter car model as an additional force to improve the passenger rid comfort.

The parameters $K_p$, $K_i$ and $K_d$ for a PID controller in an active suspension system can be obtained automatically using PID tuner in MATLAB/Simulink. The values of the controller parameters generated automatically in PID tuner are given in Table 2.

**Table 2.** Controller parameters generated in PID tuner.

| Parameter | Value |
|---|---|
| P | 104290 |
| I | 316433 |
| D | 8159 |
| N (Filter coefficient) | 3240 |

## 5. Simulation Results and Discussion

In this section, simulation results are presented using MATLAB/Simulink software to illustrate the effectiveness of the active suspension system. The performance of the active suspension system is compared with that of the passive suspension system.

Preprints.org (www.preprints.org) | NOT PEER-REVIEWED | Posted: 5 March 2026 doi:10.20944/preprints202603.0358.v1



Figures 7 and 8 show clearly how the active suspension system using PID control strategy can effectively absorb the car vibration in comparison to the passive suspension system. The sprung mass vertical acceleration $\ddot{z}_s(t)$ in the active suspension system is decreased significantly, which guarantee better passenger ride comfort. Also, the tyre deflection $z_u(t) - z_r(t)$ in the active suspension system is smaller, which guarantee better road handling ability.

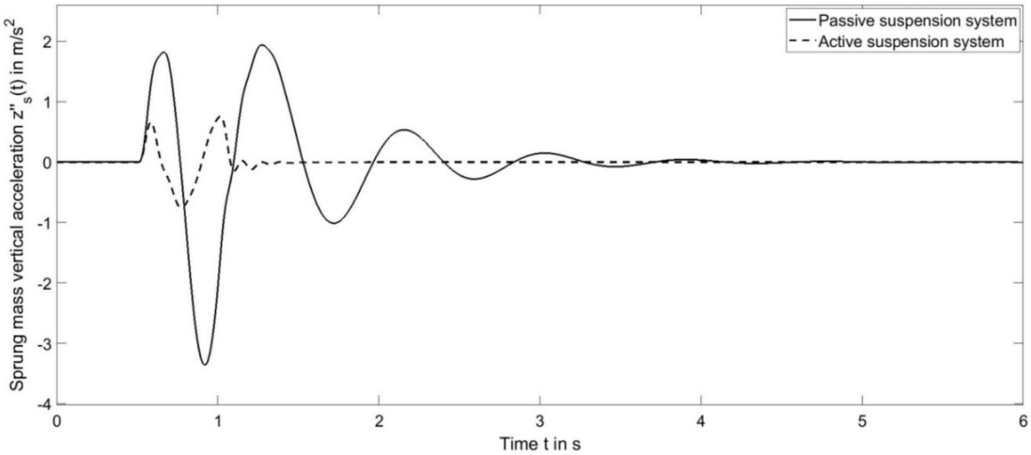


**Figure 7.** Sprung mass vertical acceleration vs. time.

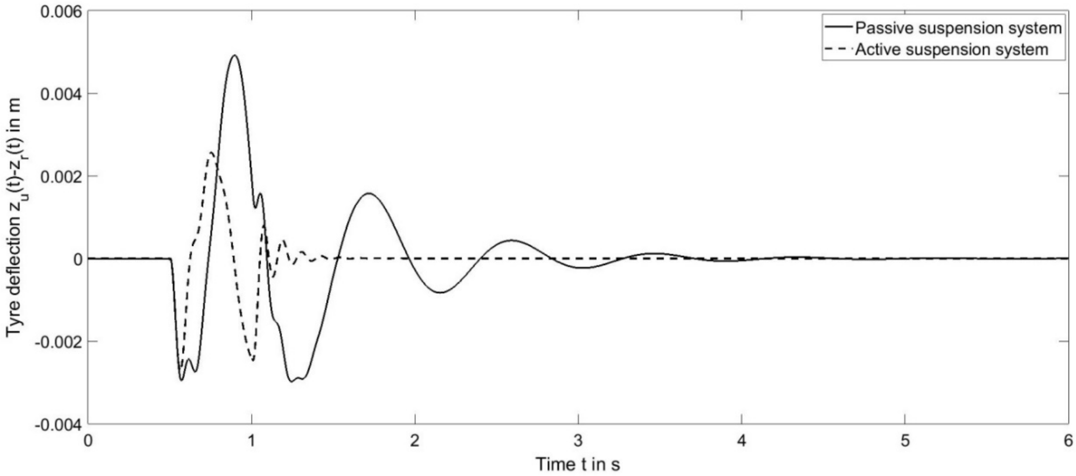


**Figure 8.** Tyre deflection vs. time.

Figure 9 shows the suspension deflection $z_s(t) - z_u(t)$ of both active and passive suspension systems. The result shows that the suspension deflection within the deflection limit $\pm 8cm$. Also, the result shows that the suspension deflection is decreased significantly in active suspension system when compared with passive suspension system.

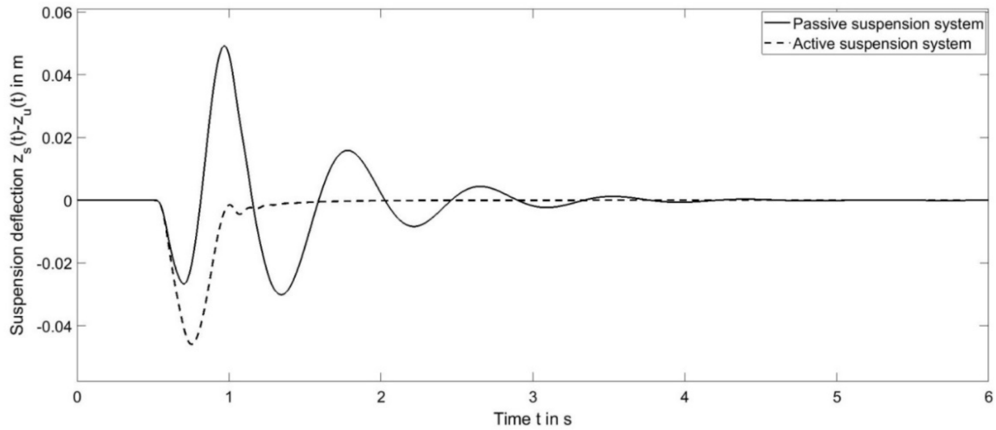


**Figure 9.** Suspension deflection vs. time.

Figures 7–9 provide a qualitative representation of the suspension system's performance. However, it is better to use quantitative representation for suspension system's performance evaluation. Table 3 shows the root mean square (RMS) values of the three performance parameters: sprung mass vertical acceleration, tyre deflection and suspension deflection for the road disturbance (speed breaker). For less RMS value indicates that the suspension system has a better performance. Also, Table 3 shows the percentage reduction in RMS values of these three performance parameters for the road disturbance.

**Table 3.** RMS values of the three performance parameters.

| | Passive suspension system | Active suspension system | % Reduction |
|---|---|---|---|
| Sprung mass vertical acceleration in $m.s^{-2}$ | 0.726 | 0.151 | 79.20 |
| Suspension deflection in m | 0.011 | 0.008 | 27.27 |
| Tyre deflection in m | 0.0011 | 0.0005 | 54.54 |

## 6. Conclusion

In this paper, the mathematical model of the active suspension system for a quarter car model with 2 DOF is derived and presented in state-space form. Then, the PID control strategy is implemented in the active suspension system to improve passenger ride comfort.

A comparison with a passive suspension system is conducted in MATLAB/Simulink. The results showed that the active suspension system improves passenger ride comfort while maintaining road handling abilities. Additionally, the suspension deflection remains within the deflection limit compared to the passive suspension system.

## References

1. PEDEN, M. World report on road traffic injury prevention. World health organization. Geneva. 2004.
2. SULTAN M.; RIESSOM, W.; ABIYOU, S. Dynamic analysis and control simulation of half car model active suspension system. M.S. thesis. Jimma, Ethiopia: Jimma University; 2019. Available from: https://repository.ju.edu.et//handle/123456789/7204
3. GEBRU, M. Road traffic accident: Human security perspective. International Journal of Peace and Development Studies. 2017, 8(2), p. 15-24. Available from: http://dx.doi.org/10.5897/IJPDS2016.0289

4. JONES, S.; TEFE, M.; ZEPHANIAH, S.; TEDLA, E.; APPIAH-OPOKU, S.; WALSH, J. Public transport and health outcomes in rural sub-Saharan Africa - A synthesis of professional opinion. Journal of Transport & Health. 2016, 3(2), p. 211-219. Available from: http://dx.doi.org/10.1016/j.jth.2015.12.005
5. SINGH, S. Critical reasons for crashes investigated in the National Motor Vehicle Crash Causation Survey. Washington, DC: National Highway Traffic Safety Administration, 2018. Available from: https://crashstats.nhtsa.dot.gov/Api/Public/ViewPublication/812506
6. SCHICK, S. Accident Related Factors. In formation Society Technologies, Project No. 027763 – TRACE, 2009.
7. WANG, H.; MUSTAFA, G.; TIAN, Y. Model-free fractional-order sliding mode control for an active vehicle suspension system. Advances in Engineering Software. 2018, 115, p. 452-461. Available from: https://doi.org/10.1016/j.advengsoft.2017.11.001
8. DU, H.; ZHANG, N. H∞ control of active vehicle suspensions with actuator time delay. Journal of Sound and Vibration. 2007, 301, p. 236-252. Available from: https://doi.org/10.1016/j.jsv.2006.09.022
9. FATEH, M. M.; ALAVI, S. Impedance control of an active suspension system. Mechatronics. 2009, 19, p. 134 -140. Available from: https://doi.org/10.1016/j.mechatronics.2008.05.005
10. HEO, S. J.; SON, S. H. Modelling of continuously variable damper for design of semi-active suspension systems. International Journal of Vehicle Design. 2003, 31(1), p. 41-57. Available from: https://doi.org/10.1504/IJVD.2003.002046
11. PAULIDES, J.; ENCICA, L.; LOMONOVA, E. A.; VANDENPUT, A. J. A. Design Considerations for a Semi-Active Electromagnetic Suspension System. Magnetics, IEEE Transactions on. 2006, 42, p. 3446 - 3448. Available from: https://doi.org/10.1109/TMAG.2006.879963
12. CHO, S. W.; JUNG, H. J.; LEE, I. Smart passive system based on magnetorheological damper. Smart Mater. Struct. 2005, 14, p. 707-714. Available from: http://dx.doi.org/10.1088/0964-1726/14/4/029
13. GILLESPIE, T. D. Fundamentals of vehicle dynamics. SAE International. 1992.
14. PRIYANDOKO, G.; MAILAH, M.; JAMALUDDIN, H. Vehicle active suspension system using skyhook adaptive neuro active force control. Mechanical Systems and Signal Processing. 2009, 23, p. 855-868. Available from: http://dx.doi.org/10.1016/j.ymssp.2008.07.014
15. ESMAILZADEH, E.; TAGHIRAD, H. D. Active Vehicle Suspensions With Optimal State-Feedback Control. International Journal of Modelling and Simulation. 1998, 18, p. 228-238. Available from: https://doi.org/10.1080/02286203.1998.11760383
16. MD YUSOF, H.; GOODALL, R. M.; DIXON, R. Active railway suspension controllers using electro-mechanical actuation technology. UKACC International Conference on Control. Coventry, UK, 2010.
17. ELMADANY, M. M.; ABDULJABBAR, Z. S. Linear Quadratic Gaussian Control of a Quarter-Car Suspension. Vehicle System Dynamics. 1999, 32(6), p. 479-497. Available from: https://doi.org/10.1076/vesd.32.6.479.4224
18. ALLEYNE, A. G.; HEDRICK, J. K. Nonlinear Adaptive Control of Active Suspensions. Control Systems Technology, IEEE Transactions on. 1995, 3(1), p. 94 - 101. Available from: http://dx.doi.org/10.1109/87.370714
19. GAO, H.; SUN, W.; SHI, P. Robust Sampled-Data H∞ Control for Vehicle Active Suspension Systems. Control Systems Technology, IEEE Transactions on. 2010, 18(1), p. 238 – 245. Available from: http://dx.doi.org/10.1109/TCST.2009.2015653
20. YOSHIMURA, T.; NAKAMINAMI, K.; KURIMOTO, M.; HINO, J. Active Suspension of Passenger Cars Using Linear and Fuzzy Logic Controls. Control Engineering Practice. 1999, 7, p. 41-47. Available from: https://doi.org/10.1016/S0967-0661(98)00145-2
21. GUCLU, R.; GULEZ, K. Neural network control of seat vibrations of a non-linear full vehicle model using PMSM. Mathematical and Computer Modelling. 2008, 47, p. 1356-1371. Available from: http://dx.doi.org/10.1016/j.mcm.2007.08.013
22. ESFANDIARI, R. S.; LU, B. Modeling and Analysis of Dynamic Systems. 2 ed. CRC Press.2014.
23. LIN, J.; KANELLAKOPOULOS, I. "Nonlinear design of active suspensions. *IEEE Control Systems Magazine*. 1997, 17(3), p. 45-59. Available from: https://doi.org/10.1109/37.588129

doi:10.20944/preprints202603.0358.v1



24. WANG, G.; CHEN, C.; YU, S. Optimization and static output-feedback control for half-car active suspensions with constrained information. Journal of Sound and Vibration. 2016, 378, p. 1-13. Available from: https://doi.org/10.1016/j.jsv.2016.05.033
25. OGATA, K. Modern Control Engineering. 5 ed. Prentice Hall. 2010.
26. CERVANTES, I.; ALVAREZ-RAMIREZ, J. On the PID tracking of robot manipulators. Systems & Control Letters. 2001, 42(1), P. 37-46. Available from: https://doi.org/10.1016/S0167-6911(00)00077-3x